Joule

CellPress

Perspective

Solar- versus Thermal-Driven Catalysis for Energy Conversion

Yufei Zhao,[1,6] Wa Gao,[2,3,6] Siwei Li,[2] Gareth R. Williams,[4] Abdul Hanif Mahadi,[5] and Ding Ma[2,*]

Today's chemical industry is a pillar of our modern society, but it heavily relies on the consumption of non-renewable fossil fuels. The reaction conditions required to drive most of the chemical processes require high energy input, resulting in the consumption of significant amounts of dwindling reserves of fossil fuels. Therefore, more sustainable pathways are much sought after to reduce the dependence on fossil fuels and ameliorate the effects of climate change. Inspired by photosynthesis and its ability to convert CO_2 and H_2O to hydrocarbons, this Perspective focuses on recent advances in catalytic small-molecule activation and conversion. It will consider reactions of C-H (CH_4, benzene), C=O (CO and CO_2), N≡N bonds, and other fine chemicals syntheses (e.g., C-C and S-S bond coupling), driven by either solar or thermal energy. The paper also discusses the future opportunities and challenges by highlighting some strategies for the development of efficient solar or thermal catalysis processes.

Introduction

Since the first industrial revolution in the 18th century, when manual production began to be mechanized, coal and oil-based fossil fuels have been crucial for the development of new technologies in numerous industries (the chemical industry, automotive industry, electrical industry, etc.). However, over the past two centuries, the consumption of fossil fuels has created numerous problems, including climate change (CO_2 emissions) and environmental pollution (NOx, SOx, volatile organic compounds [VOCs], and particulate matter [PM]).[1] Furthermore, the global supply of fossil fuels is dwindling. New sustainable and green solutions to address the increasing global energy demands and the need to protect the environment are highly desirable for both the economy and society. Since fossil fuels originate from photosynthesis, in which CO_2 and H_2O are used as raw materials for the synthesis of hydrocarbons, the direct use of solar energy could potentially resolve the above issues.

Photocatalysis utilizes solar energy to accelerate key reactions such as water splitting for hydrogen production and the photoreduction of CO_2 into hydrocarbons. Very recently, the advances on photocatalysis have enabled exciting development in CO, CO_2, or N_2 hydrogenation to generate high-value hydrocarbons (olefins and alcohols) or NH_3 under flow conditions.[2] By rational design of the reactor and the assistance of the external field (thermal, solar, or electronic field), some solar-driven catalytic processes such as photo, photoelectro or photothermal, and plasmonic catalysis have emerged as promising approaches for energy conversion, where solar-to-fuel conversion efficiency has increased rapidly from less than 1% to ~14% in the past few years.[3] Moreover, solar-driven catalysis has shown significant progress, where their activities have increased from μmol/gcath to mmol/gcath or mol/gcath in the past 5 years.[4,5] This rapid improvement demonstrates a strong confidence to the scientific and industrial area that solar routes are now competitive with traditional thermal catalysts, especially in C-H, C=O, and N-N activation

Context & Scale

Thermal catalytic technologies currently available for today's chemical industry (e.g., Haber-Bosch ammonia synthesis) require high temperatures (>400°C) and pressures (many atmospheres) to achieve viable N_2 conversions. Various green alternative technologies are now being pursued for N_2 and other small-molecule (such as CH_4 and CO_2) activation and conversion. Solar-driven catalysis is particularly attractive because of the abundance of solar energy on Earth as well as its high selectivity under mild reaction conditions, potentially providing an alternative green and sustainable route for energy conversion and/or storage. This Perspective focuses on the recent advances in small molecules (CH_4, benzene, CO, CO_2, and N_2) and fine chemical synthesis by either solar or thermal catalysis and presents a critical assessment of the advantages and disadvantages of solar-driven catalysis, as compared with the traditional thermal catalysis, in terms of catalytic activity, selectivity, and stability. A classification of various mechanisms between solar-driven and thermal catalysis will be clearly summarized to provide a systematic understanding on the chemical bonding activation and reaction and resulting in a new vista for future research on catalytic energy conversion/storage.

processes such as CH_4 conversion, benzene activation, CO_2 or CO reduction, and N_2 fixation.

In this article, we will compare and contrast traditional thermal catalytic processes with the emerging solar-driven approaches, with specific attention to the reaction mechanisms of the above processes. The ability of the catalysts to give efficient energy conversion in reactions of small molecules (CH_4, benzene, CO, CO_2, and N_2) and fine chemical synthesis will be discussed in terms of catalytic conversion, efficiency, and selectivity. The authors hope that this perspective will focus on the potential of solar-driven catalysis and encourage the industrial or scientific researchers in this exciting area.

A Brief Overview of Solar-Driven Catalysis

Photocatalysis and Photoelectrocatalysis

A photocatalyst with a suitable band gap can absorb solar energy to generate photo-induced charge carriers (electron-hole pairs). These carriers need to be separated and transferred to the catalyst surface to be active. Inevitably, there will be some combination of the pairs during the transportation process, which hampers the efficiency. Surface-adsorbed reactants can react with the charge carriers, and the valance and conductive band energies provide a driving force for oxidation and reduction reactions, respectively. The relative band structure (as determined by the atomic make-up of the catalyst) further affects their oxidation and/or reduction ability. Because of its ability to exploit unlimited solar energy and the potential to drive thermodynamically unfavorable chemical reactions forward (Figure 1), photocatalysis can comprise a low-emission route to H_2O splitting,[6] CO_2 reduction,[7] N_2 fixation,[8,9] and fine chemical synthesis,[10] as well as photocatalytic dye degradation in solid-liquid, solid-gas, or solid-liquid-gas systems.[11] To ensure an effective catalytic process, often co-catalysts or external fields are further required to increase the migration efficiency of electrons and holes.

The first work on photoelectrochemical (PEC) catalytic water splitting was reported by Boddy in 1968 over semiconducting TiO_2 using a mercury arc lamp.[12] Later in 1972, Fujishima and Honda proposed the visible light splitting of water into O_2 and H_2 without any external voltage over a semiconductor.[13] Under the assistance of electron field, light photons stimulate the generation of electron-hole pairs, with a highly efficient separation and migration of charge carriers to the electrode interface. The anode or cathode electrode surface catalyzes water oxidation/reduction with the carriers. Over the past 45 years or so, a number of key developments in the design of efficient PEC-based cells have been reported.[14] In addition to photovoltaic (PV) cells based on silicon solar panels, dye-sensitized solar cells (DSSCs),[15] perovskite solar cells,[16] and various other types have been developed. All of these can directly absorb solar energy and convert the photons into free charge carriers for the generation of electricity (Figure 1). Because of their low cost and efficient energy production, PV-based cells are now competitive with fossil fuels. Recently, Grätzel and co-workers have reported a tandem PV system based on perovskite solar cell-bifunctional water splitting layered double hydroxide (LDH) electrocatalysts for water splitting, with a solar-to-H_2 efficiency of 12.3%.[17] This exciting advance in the solar-to-fuel energy conversion efficiency is closing the gap to the industry requirements, providing an exciting pathway for the solar energy conversion.

Photothermal Catalysis

Recently, photothermal catalysis processes have been shown to provide a potential alternative to traditional thermal catalysis. Through light irradiation, especially of

[1]State Key Laboratory of Chemical Resource Engineering, Beijing University of Chemical Technology, Beijing 100029, China

[2]Beijing National Laboratory for Molecular Sciences, College of Chemistry and Molecular Engineering, and BIC-ESAT, Peking University, Beijing 100871, China

[3]Key Laboratory of Urban Agriculture (North China), Ministry of Agriculture, College of Biological Science and Engineering, Beijing University of Agriculture, Beijing 102206, China

[4]UCL School of Pharmacy, University College London, 29–39 Brunswick Square, London WC1N 1AX, UK

[5]Center for Advanced Material and Energy Sciences, Universiti Brunei Darussalam, BE1410 Brunei Darussalam

[6]These authors contributed equally

*Correspondence: dma@pku.edu.cn

https://doi.org/10.1016/j.joule.2019.03.003

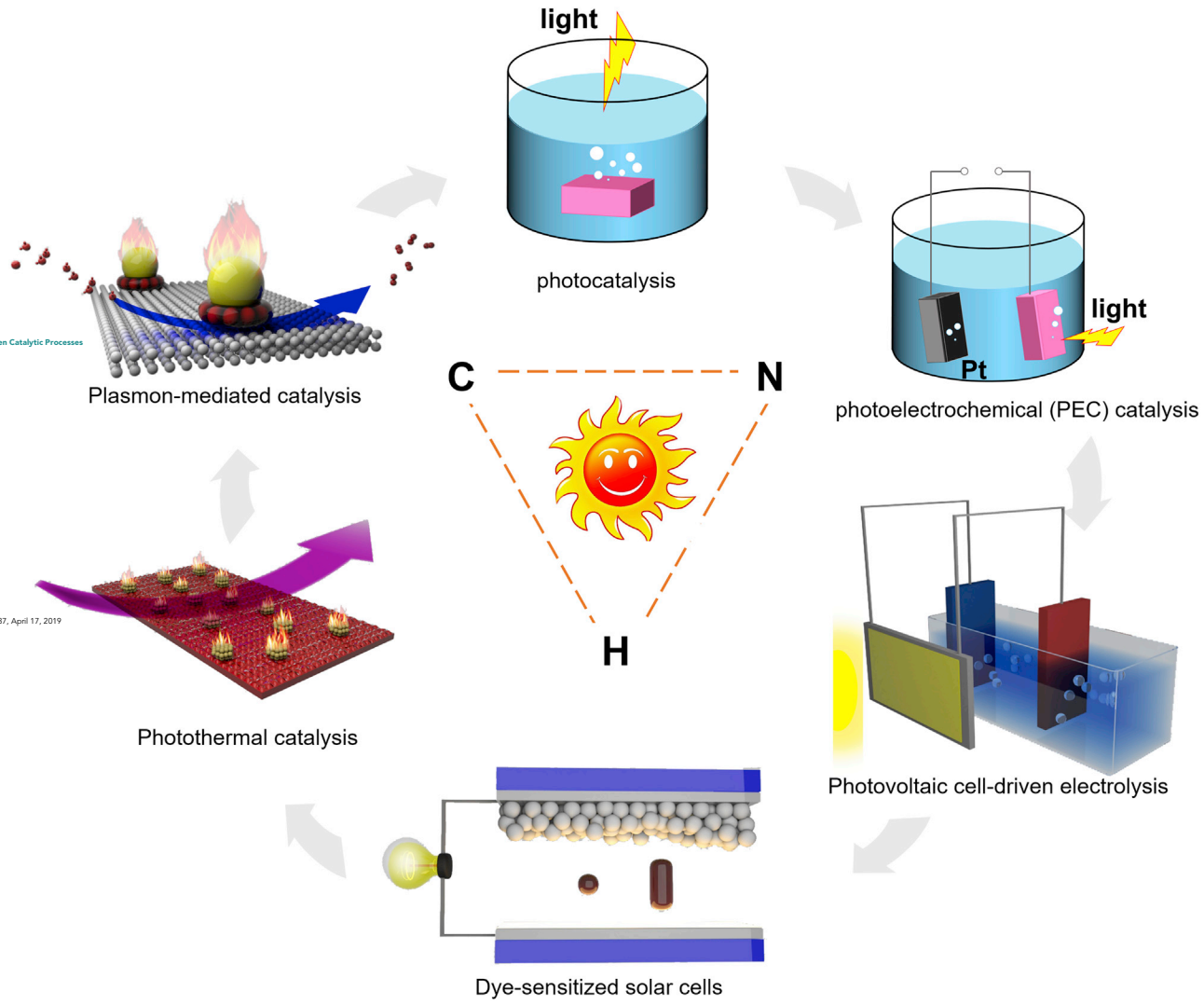

Figure 1. Solar-Driven Catalytic Processes

black powder samples, visible and near-infrared light energy can generally dissipate into heat (temperature), providing nearly the same amount of energy as conventional catalytic reactions.[18] Because of the high energy efficiency of this photothermal effect, the surface temperature can reach 300°–500°C or even higher,[19] providing enough energy to drive thermodynamically unfavorable reactions such as CO_2 reduction[20] and N_2 hydrogenation[21] processes (Figure 1). It should be noted, however, that the real temperature of the photo-induced local hotspots may be much higher than that tested by the thermal sensors, particularly at a nanoscale level; thus, it is still a challenge to study the real thermodynamics and kinetics of photothermal catalysis for further understanding of the catalytic mechanism. Besides the traditional photothermal catalysis (with only photo-induced thermal effect), some photocatalytic effect (with the formation of photoinduced carriers) can simultaneously exist with thermal effect (heat effect); therefore, the synergy between the photocatalytic and thermal effects in the photothermal catalysis under the solar spectrum irradiation still needs to be explored in detail.[5] This synergistic effect has been observed on photocatalysis of TiO_2 and thermal catalysis of CeO_2

when using TiO_2/CeO_2 nanocomposites in the gas-phase oxidation of benzene under light irradiation. The CO_2 formation rate of the TiO_2/CeO_2 nanocomposite is 36.4 times higher than the conventional photocatalytic process (at room temperature).[22] The novel strategy not only makes up for the disadvantages of TiO_2 photocatalysis, which on its own is unable to completely oxidize the benzene (only under light irradiation), but also overcomes the energy-consuming problem of single thermal catalysis that must operate at a higher temperature by using an additional heater, exploring the synergetic effect between the individual photoinduced carriers and the photoinduced heat in the photocatalytic-thermal catalysis.

Plasmon-Mediated Catalysis

Plasmonic metal (Au, Ag, Cu, etc.) nanocrystals with wide light absorption ranges can photogenerate high-energy electrons (so-called "hot electrons") when oscillations of the conduction electrons are excited under light.[23] Compared with the direct photoexcitation process, the hot electrons produced by non-radiative decay of localized surface plasmons is much more energetic than the common intensity of traditional photocatalysis.[24] When the metal is in contact with an n-type TiO_2 semiconductor, a Schottky barrier around the interface promotes electron transfer and suppresses the combination of charge carriers. These are different from traditional co-catalyst-loaded semiconductor systems because plasmonic metal-semiconductors such as Au-TiO_2 can reach theoretical incident photo-to-current conversion efficiency (IPCE) of around 26%, much higher than the traditional photocatalytic IPCE of around 1%, serving as a highly promising candidate for solar energy exploitation.[25] Both electrocatalytic water oxidation[26] and plasmonic-catalytic styrene hydrogenation into ethylbenzene[27] have been reported by dint of the plasmonic effect. In addition to the above-mentioned photoexcited plasmonic effects, a thermal catalytic effect cannot be ignored since these plasmonic metals have been widely used as supported noble metal thermal catalysts in thermal catalysis. When considering plasmonic metal-semiconductor systems, the dual-functional roles of metals (photoexcited plasmonic and surface catalytic effect) should be separately discussed. For example, Zheng and co-workers prepared a series of Au-modified CeO_2 samples with various Au loading amounts (0.25–1 wt %) and particle sizes (3–20 nm) to explore the surface plasmon resonance photoabsorption, charge separation, resonant energy transfer, and surface catalysis in the aerobic oxidation of propylene reaction.[28] It was found that photoexcitation and surface catalysis presented opposite correlation on Au nanoparticle size and co-determined the final photocatalytic performance. Hence, finding optimal Au particle sizes (6–12 nm) that maximize the balance between the plasmonic and catalytic roles over metallic nanostructures would be ideal for the further rational design of efficient plasmonic metal-semiconductor systems. It is very likely that plasmon-assisted catalysis will lead to further breakthroughs in the future.

A Short Overview of Thermal-Driven Catalysis

The modern chemical industry is founded on the basis of using thermal heterogeneous catalysis, powered by coal, oil, and natural gas, for the large-scale synthesis of NH_3, olefins, hydrocarbons, and fine chemicals (Figure 2).[29] Considering the highly successful NH_3 synthesis process as an example, pressures and temperatures of around 20–40 MPa and 400°C–600°C, respectively, are required. This consumes 2% of global energy output, with vast amounts of CO_2 released during the reaction. Such high energy is required to overcome the activation barrier for the rate-determining step of the reaction, fission of the $N\equiv N$ bond (945 kJ mol^{-1}). During the thermal catalytic process, N_2 molecules accept electron density from the valence orbitals of the transition metals (Fe and Ru) used for catalysis into their antibonding

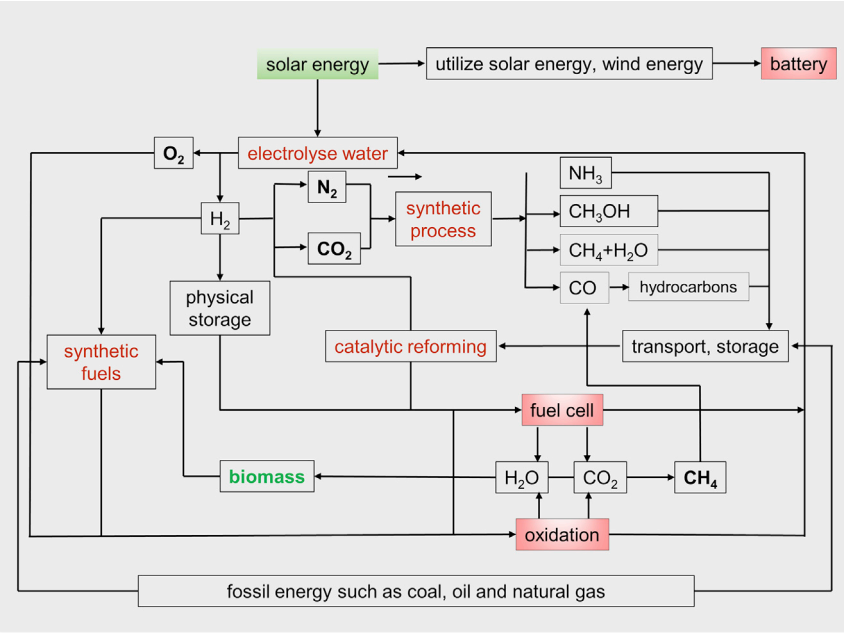

Figure 2. Thermal-Driven Catalysis Process

This is mainly based on traditional fossil resources (as coal, oil, and natural gas). Partly revised from Schlögl et al.,[29] with permission from Wiley-VCH.

π-orbitals. This weakens the N≡N bond, resulting in further hydrogenation to *NNH, and ultimately the formation of NH_3. The very significant energy input required to drive the process and the high cost of the H_2 feedstock demands the development of more sustainable photo- and/or electro-driven N_2 fixation pathways or the adaption of the enzymatic process from the nitrogen cycle.[30]

During the NH_3 generation and coal-to-oil (Fischer-Tropsch synthesis, FTS) industrial process, H_2 has been widely considered as industrial blood in the hydrogenation reaction. Because of the most abundant resource of hydrogen, H_2O is the ideal source of H_2. However, thermal water splitting method into H_2 is impossible since it requires temperatures of above 1,000°C. Until now, the most successful H_2 generation process from traditional catalytic routes is the water gas shift ($CO + H_2O = CO_2 + H_2$; WGS) reaction by using CO, forming CO_2 as a byproduct. By using a noble metal (Au) or Cu as the main catalyst, the dissociation of H_2O occurs on the metal catalyst surface to form H and OH species, with the OH reacting with CO to yield CO_2 and H, followed by the coupling of H-H for the desorption/formation of H_2.[31] This process produces H_2 but with the inevitable evolution of an equal mole of the greenhouse gas CO_2. Alternatively, by virtue of photo/electro-catalysis, H_2O can be directly split into H_2 and O_2 from cathode and anode under mild conditions, and the two products can be easily separated using earth-abundant semiconductor or electrocatalyst materials.

Solar and Thermally Catalyzed Small-Molecule Conversion

C-H Activation

CH_4, a symmetrical molecule without any reactive functional groups, contains a very strong C-H bond of 434 kJ mol^{-1} and thus has low chemical reactivity.[32] Only a deep vacuum ultraviolet (VUV) light below 140 nm in wavelength can excite CH_4 via electronic transitions. Thermodynamically, the direct non-oxidative coupling of methane

Table 1. Characteristics of Solar and Thermal Conversion of Methane

Conditions	Solar		Thermal	
	Direct	Oxidation	Nonoxidative	Oxidative
Temperature	room temperature	~400°C, RT (only H_2O_2), RT (PEC)	>700°C	700°C–850°C, RT (only H_2O_2)
Thermodynamics	limited	not limited	limited	not limited
Catalysts	Zn^+/ZSM-5, GaN, etc.	Ni/SiO_2, Rh/TiO_2, FeO_x/TiO_2	Mo/ZSM,Fe/ZSM, Fe©SiO_2	Li/MgO, Sr/La_2O_3, Na/W/Mn/SiO_2, Fe-CN
Main products	C_6H_6, C_2H_6, H_2 etc.	CO_2, CO, H_2, C_2H_4, CH_3OH	C_6H_6, H_2, C_2H_4 etc.	C_2H_4, C_2H_6, CO, CO_2, H_2O, CH_3OH
Conversion	~300–9,800 μmol/gh	1–330 μmol/gh	~0.5 mol/gh (14.5 L/gh)	>0.1 mol/gh
Main drawback	catalysts synthesis, low conversion	low conversion and selectivity	coke formation, stability issues, harsh operating conditions	overoxidation, stability issue

(NOCM) is much more unfavorable than methane activation with oxidation (O_2, CO_2, etc.). Therefore, direct coupling of CH_4 requires a very high temperature to overcome the activation energy barrier.[33] A recent breakthrough in thermal CH_4 activation was reported by Bao and co-workers.[34] By using a single-Fe site/silica matrix as the catalyst at 1,090°C, CH_4 conversion of 48.1% was obtained at a CH_4 space velocity of 21,400 mL/g_{cat}h, with ethylene selectivity of 48.4%. Other byproducts comprising aromatics and H_2 were also obtained through this direct non-oxidative process. The Fe site embedded within the silica support activated the C-H bond and generated methyl radicals for further C-C coupling.

Compared with the harsh conditions required for thermal CH_4 activation, photocatalytic CH_4 conversion requires much milder conditions. The first photocatalytic NOCM was reported in 1998 by Yoshida and co-workers.[35] After 18-h treatment with UV light over silica-alumina and alumina in a closed quartz reaction vessel, CH_4 (100 μmol) was converted to an extent of 5%, with high selectivity for ethane formation (60%) and avoiding the generation of CO_2 and CO. This was achieved at room temperature. The activation of CH_4 has further been investigated by Chen and co-workers using Zn^+-modified ZSM-5 zeolite catalysts under mercury or sunlight irradiation at room temperature.[36] Up to 24% CH_4 conversion could be obtained after 8 h, at a rate of 10 mmol/gh and with >99% selectivity for ethane and hydrogen products. The active 4s electron of Zn^+ can be photoexcited into empty C-H antibonding orbitals on CH_4, driving coupling reactions. Chen's sunlight-driven CH_4 conversion was the first example of solar-catalyzed CH_4 conversion under environmental conditions. Further, Ga^{3+}-modified zeolites[37] and GaN-based UV-responsive photocatalysts[38] also permit the direct conversion of CH_4 to hydrocarbons and benzene at room temperature. Very recently, a new PEC approach for CH_4 oxidation to CO over Ti^{3+} doped atomic-layer-deposition-grown TiO_2 has been reported for the CO production with over 80% selectivity in all products (CO, O_2, and carbonate, etc.).[39] Details of typical activities can be found in Table 1. It is extremely promising that, using sunlight without any further energy, CH_4 can be directly converted into high-value products, although the reaction rate is still several orders of magnitude lower than thermally catalyzed processes.

It has also been found that, using other oxidation agents (H_2O_2, H_2O, and CO_2), CH_4 can be efficiently oxidized into methanol and long-chain hydrocarbons under a combined thermal- or solar-driven catalytic process.[32] Recent developments in solar-driven photothermal CH_4 oxidation have allowed the generation of CO_2 and H_2 using composite materials (Ni/SiO_2 and Rh/TiO_2).[40,41] Under solar irradiation, the surface temperature of the catalysts can reach up to 400°C–500°C. An H_2O_2 strategy

based on single-atom catalysts permitted CH_4 conversion to CH_3OH under mild conditions (room temperature and 2 MPa), providing an exciting route to CH_4 conversion.[42] Furthermore, photocatalytic (one sun) conversion of CH_4 to CH_3OH with a high selectivity of over 90% in alcohols has been reported over FeO_x-TiO_2 using H_2O_2 at room temperature and pressure. This photocatalysis technology that utilizes photons instead of thermal energy to drive molecular activation and/or conversion at much milder conditions than was previously possible.[43] However, efficient conversion of CH_4 into more high-value products remains a challenge. With the development of nanoscience and technology for developing efficient nanoscale catalysts, conditions for thermal CH_4 oxidation could become milder and economical, while solar-driven catalytic CH_4 oxidation becomes more efficient with retaining advantages in selectivity under mild conditions.

Derivatives of benzene (e.g., phenol, aniline, and nitrobenzol) are important organic intermediates widely used as precursors of dyes, polymers, plastics, pharmaceuticals, and agrochemicals. For the synthesis of phenol, the multi-step cumene process is widely used in industry; this operates at 3 MPa and 250°C,[44] uses stoichiometric reducing agents, and creates large amounts of environmentally toxic waste. In attempts to resolve these issues, the one-step amination of benzene with ammonia to generate aniline and one-step oxygenation of benzene to phenol have been extensively studied.[45] However, these processes are typically carried out under extreme conditions and produce very low yields and selectivities for aniline and phenol formation. This is due to the inherent inertness of the aromatic ring C_{sp2}-H bonds. Recent developments have suggested that it is possible to operate at milder conditions. Wang et al. achieved H_2O_2-mediated ring hydroxylation of various arenes into the corresponding phenols using a heterogeneous catalyst comprising V-ZSM-22.[46] The reaction was at 80°C with the assistance of CH_3CN and H_2SO_4. For benzene hydroxylation, the phenol yield is 30.8% (selectivity > 99%). Such high activity is associated with a unique non-radical hydroxylation mechanism arising from the diperoxo V (IV) state created *in situ*. This provides a promising approach toward robust heterogeneous catalysis for selective H_2O_2-based hydroxylation of C_{sp2}-H bonds. However, a greener route for the above reaction is still to be desired if H_2O can be used as oxidation.

Solar-driven photocatalysis using environmentally benign reactants such as water or molecular oxygen is within reach. Sano and co-workers described a new methodology, which can be used to attain high photocatalytic activity for partial oxidations using TiO_2. This approach used layered silicate clay minerals with different interlayer ions (protons intercalated in $H_2Si_{14}O_{29}$ clay or Na intercalated in $Na_2Si_{14}O_{29}$ clay) and O_2 saturated water as the only oxidant. They achieved a phenol production of 119 and 13 μmol at ca. 80% benzene conversion.[47] The phenol-philic adsorbent derived from the layered protons intercalated silicate ($H_2Si_{14}O_{29}$) can selectively adsorb phenol from an aqueous benzene solution, preventing overoxidation on TiO_2. The combination of layered silicates with TiO_2 thus opened a door to green fine-chemical synthesis.

Tung and co-workers developed an alternative strategy termed hydrogen-evolution cross-coupling reactions (HCCRs) for benzene amination and hydroxylation. This was achieved via a combination of photocatalysis and cobalt-complex catalysts.[48] Without any sacrificial oxidant, the dual-catalyst system produced aniline directly from benzene and ammonia, and phenol from benzene and water. In both cases, H_2 was evolved, and the reactions could be performed at room temperature while still giving excellent yields and selectivities.

The above examples of solar-driven C-H activation allow high yields, high selectivity, and catalyst reusability in the synthesis of hydrocarbons and fine chemicals. They are thus highly attractive for industrial applications, given that thermal catalysis usually requires harsh and expensive reaction conditions. The formation of active species *in situ* and new reaction mechanisms play a key role in such high performance.

C=O Activation

Achieving C=O activation of CO_2 and CO is a crucial requirement for halting and reversing the progress of climate change.[49,50] Using nanoparticles of 3d transition metals (Fe, Co, Ni, Ru, Rh, Pd, Ir, and Pt) supported on SiO_2 or Al_2O_3 as solar-driven catalysts, CO_2 can be hydrogenated into CH_4 and/or CO.[49,51] Compared with a photosynthesis process using H_2O as a reductive agent, the activity of photothermal CO_2 hydrogenation (approximately several mol/gh) is 5–10 orders of magnitude higher than that of photocatalytic CO_2 reduction with H_2O as the proton source ($\sim 10^{-9}$ mol/gh). The main reason underlying this difference is the much higher solar energy utilization efficiency with the photothermal effect. Since catalyst surface temperatures reach up to 300°C–500°C,[19] H_2 dissociation can be achieved. Comparably, the rate-determining step for photocatalytic CO_2 reduction by H_2O is the formation of H atoms from water splitting. The direct use of H_2 as the reductive source gives solar-driven CO_2 hydrogenation nearly the same product yield as traditional thermal catalysis, which provides an efficient pathway for the solar-driven catalysis.[20] However, the product from photocatalytic CO_2 hydrogenation is mainly CH_4, and routes to more high-value hydrocarbons are still required.

Inspired by the use of traditional thermal catalysts for the valuable hydrocarbon synthesis through C-C coupling over Fe- or Co-containing Fischer-Tropsch (FT) catalysts, solar-driven CO_2 hydrogenation processes have been reported with products varying from CO to CH_4 and also valuable hydrocarbons (with >35% selectivity for C_{2+} hydrocarbons).[52] This is achieved by controlling the reduction temperature of the CoFeAl-LDH catalyst precursor from 300°C to 700°C.[52] X-ray absorption fine structure (XAFS) revealed that FeO_x was the first phase to migrate to the surface of the nanosheets with a reduction temperature lower than 400°C. Increasing the reduction temperature to 600°C resulted in the co-existence of FeO_x and CoO_x nanoparticles supported on the nanosheets. If the reduction temperature is increased above 600°C, a CoFe-alloy phase is formed, which has a surface photothermal effect at 320°C under light irradiation that enables C-C coupling for the CO_2 hydrogenation to hydrocarbons. This strategy provides a new route to solar-driven hydrocarbon synthesis from a CO_2 feedstock. Without using solar energy, the CO_2 conversion profiles are the same with the temperature provided only from heat, indicating this photothermal CO_2 hydrogenation catalysis is nearly the same as thermal catalysis, with the only difference being that the energy is sustainable and clean in the latter case. However, to generate alkenes instead of alkanes, further work is needed to control the electronic structure of the catalysts.

Recently, CO hydrogenation to hydrocarbons (FT synthesis) has attracted extensive attention, especially in China.[53–55] Ma and co-workers developed a solar-driven FT to olefin (FTO) process over an Fe_5C_2 catalyst, leading to an olefin/paraffin (o/p) ratio of 10.9 and low CO_2 selectivity (18.9%) with CO conversion of ~49% (Figure 3).[56] Interestingly, under traditional thermal reaction (the temperatures reached the photo-driven catalyst temperature around 500°C; Figure 3B), the CO conversion reached 80.5%, but the dominant product was CH_4 with high selectivity of 95.1% in hydrocarbons and CO_2 (36.0% of all products) and a negligible o/p ratio (0.1). It is interesting to note that there are different product distributions under thermal and photo-driven

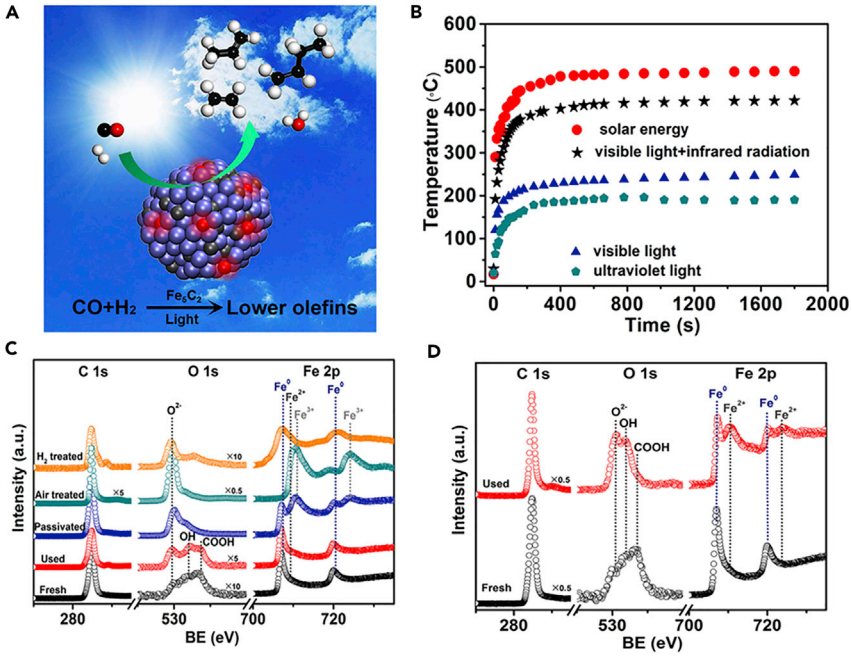

Figure 3. Solar-Driven C=O Activation

(A) Illustration of the solar-driven products obtained from Fe_5C_2 catalyst.

(B) Monitoring of the catalyst bed temperature of Fe_5C_2 under photo-irradiation.

(C) *Ex situ* X-ray photoelectron spectroscopy (XPS) spectra of the Fe_5C_2 catalyst under different treated conditions.

(D) *Ex situ* XPS spectra of the fresh Fe_5C_2 catalyst and after traditional thermal reaction.

Reproduced from Gao et al.,[56] with permission from Elsevier.

reactions (even at the same temperature range). This indicates that solar-driven FTS is mechanistically different from traditional photothermal catalysis (with only heating effects) or thermal catalysis. Under solar irradiation, the surface of the Fe_5C_2 catalyst was spontaneously partly decorated by oxygen atoms formed *in situ* (Figure 3C), which can modify the local electronic structure and the optical band gap of the surface, leading to easier C_2H_4 desorption and avoiding further over-hydrogenation to C_2H_6, resulting in a high selectivity to olefins. Compared to the traditional thermal reaction, the Fe_5C_2 surface was heavily oxidized to oxides with a significant presence of Fe^{2+} species (Figure 3D), resulting in over-hydrogenation performance of olefins. The excited-state energy of C_2H_6 (−1.31 eV, photo-driven reaction) is also suppressed on the O-decorated Fe_5C_2 surface over ground-state energy of C_2H_6 (−1.71 eV, thermal reaction) as calculated from excited-DFT, explaining the preferred products of olefins on excited state (photo-driven FTS) over the formation of alkane on ground state (thermal FTS). The enhanced photothermal catalysis arises for several reasons: (1) the presence of Fe_5C_2 in the oxygen-decorated catalyst, which is responsible for light-heat transformation and (2) the existence of a small amount of FeO_x species on Fe_5C_2, which under light absorption becomes stimulated and interacts with the reactants, resulting in a different reaction path and different product distribution. Thus, solar-driven reactions provide a new suite of catalytic routes to change reagent reactivity or product selectivity and provide a new view on the traditional photothermal or thermal catalysis.

Although great achievements have been made in using solar energy instead of heat, the following issues remain to be addressed: (1) even though similar activity and/or

selectivity can be obtained by using solar instead of thermal energy, more work is needed to understand and control the reaction mechanisms of solar-driven processes under this photo-driven excited state; (2) since some photothermal catalysts use semiconductor supports, the contribution of photothermal and photocatalytic (photoinduced electro and holes) effects to the overall catalytic process is still not clear and needs to be explored in more detail.

N≡N Activation

Since the Fe-based Haber-Bosch ammonia synthesis requires H_2 and very high energy input, there is a need for technologies with milder reaction conditions (below 400°C, and <2 MPa). The possibility of using solar energy to drive this process is very attractive.[57] Recently, the exploration of alternatives to the traditional Fe-based catalysts has been developed by tuning the interaction between a support and N_2 molecules. Hosomo and co-workers reported using electride ([CaAlO]-e) as a support, and as a result of its high electron-donating power and chemical stability, Ru-electride worked as an efficient NH_3 synthesis under 400°C and 1 MPa.[58] Furthermore, intermetallic LaCoSi was also reported to be potent here, showing a superior activity for NH_3 synthesis with a rate of 1,250 μmol/gh at 400°C and 0.1 MPa.[59] Several new catalysts, such as transition metals or its nitride-LiH composites,[60] and metal imides[61] have also been reported recently by Chen and co-workers, giving promising performances in the temperature range of 100°C–320°C and at atmospheric pressure. Besides thermal catalysis, Zhang reported photothermal N_2 hydrogenation over Ru-K-TiO_2 at atmospheric pressure using the surface plasmon resonance effects of Ru nanoparticles.[21] The catalyst surface temperature was found to reach 360°C in 13 min, and an NH_3 yield of 112.6 μmol/gh was obtained with a gas flow of 6 mL/min. This is 6.7 times greater than the yield obtained with Ru-K-MgO under the same thermal conditions.[21] This purely solar-driven NH_3 synthesis approach offers a renewable way for N_2 hydrogenation.

The H_2 used in standard NH_3 synthesis is expensive, and thus the use of H_2O as an alternative proton source has been explored. Many ultrathin 2D materials (BiOBr,[8,62] Mo-doped, $W_{18}O_{49}$[63]) and TiO_2 catalysts[64] with photocatalytic activity have been reported to be potent in N_2 fixation. These species have surface defects that provide coordinated unsaturated metal sites for efficient reactant adsorption. Ultrathin LDH nanosheets have attracted particular attention in this context mainly because of the abundance of surface defects.[65] Their synthesis can be easily scaled up, and their flexibility of chemical composition allows them to be efficient in N_2 fixation under visible light (even at 500 nm). This has been reported to give an NH_3 yield of ~74 μmol/gh using H_2O as a proton source.

The nitrogenase enzyme comprises an activating MoFe-protein to provide an active site for the initial binding and activation of an N_2 molecule, while the other catalytic Fe-protein provides a site for the decomposition of adenosine triphosphate (ATP), thereby releasing an electron for N_2 reduction (Figure 4A). Such a "work-in-tandem" system between the two proteins provides a talent for N_2 fixation process. Artificial systems working on the same principles can also be prepared.[66] One example of this is plasmonic Au loaded on O-deficient ultrathin TiO_2 nanosheets, which gave an excellent N_2 fixation activity under visible light by using methanol as hole sacrificial agent (Figures 4B–4D).[66] NH_3 formation over this catalyst can be divided into four steps. First, the oxygen vacancies provide sites for N_2 adsorption. Under visible light irradiation, hot electrons formed from Au particles are transferred to the conduction band of the TiO_2 support. These hot electrons are then trapped in the defect sites and enter the anti-bonding orbitals of N_2, resulting in the formation of NH* and

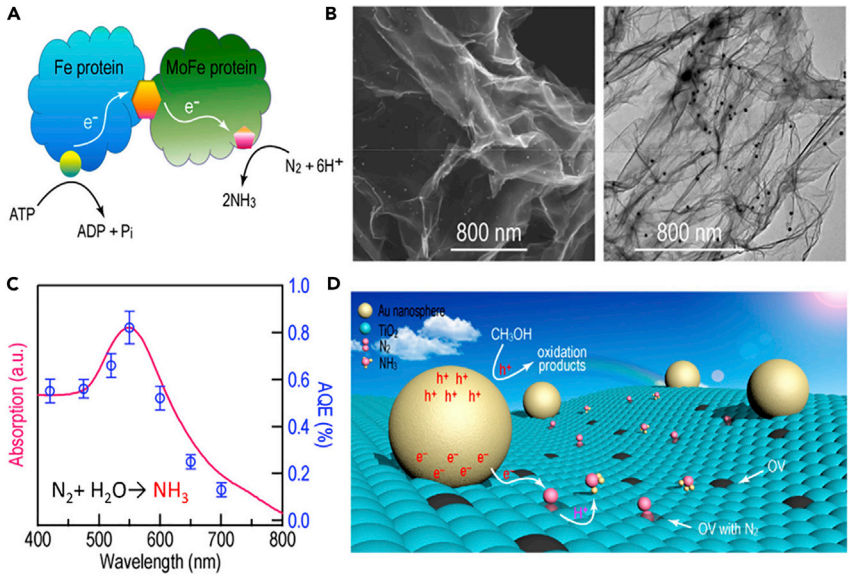

Figure 4. Photocatalytic N≡N Activation

(A) Schematic illustrating the "working-in-tandem" mechanism of the nitrogenase with the Fe protein and MoFe-protein in biological N_2 fixation.

(B) SEM and TEM images of Au/TiO_2.

(C) Absorption and ammonia evolution action of Au/TiO_2.

(D) A schematic illustration of the plasmonic N_2 photo fixation mechanism. Reproduced from Yang et al.,[66] with permission from American Chemical Society.

NH_3. The "hot holes" generated from Au are consumed by the methanol. The quantum efficiency was determined to be 0.82% at 550 nm, and the photocatalytic NH_3 synthesis activity can even extend to 700 nm with the assistance of the sacrificial agent (Figure 4C). However, use of methanol to aid the process is not economical, and finding a more efficient method for photocatalysis is still a challenge.

In order to further increase the charge separation efficiency of the catalyst, a TiO_2-Au-amorphous TiO_2 sandwich structure was used to generate photoelectrode arrays.[67] It exhibits efficient activity in solar-driven PEC N_2 reduction, without any sacrificial agent. The PEC system exhibited an NH_3 generation rate of 13.4 nmol cm^{-2} h^{-1}, 2.6 times greater than the bare TiO_2 array. This enhanced activity arises from the electric field intensity of TiO_2-Au, which is 10 times stronger than bare TiO_2. With the assistance of the plasmonic effect, other small molecules such as CH_4[68] and CO_2[69] can also be activated and transferred into ethane and CH_4, respectively, under solar light irradiation.

It should be noted that the N_2 fixation products (NH_3 or NH_4^+) are generally detected by the Nessler method or nuclear magnetic resonance (NMR) spectra; however, there is a possibility of misinterpretation of product detection because of using some N-containing catalysts (such as CoMoN-, CN-, VN-, or NO_3-containing catalysts or some N-containing surfactants during the synthesis process). Xu and co-workers explored the active phases in N_2 electroreduction over vanadium oxides, oxynitride, and nitride species using *ex situ* photoelectron spectroscopy, operando X-ray absorption spectroscopy, isotopic labeling experiments with ^{15}N-labeled N_2, and DFT, which provide the N_2 reduction mechanism clearly.[70] We believe that with the benefit of *in situ* and operando characterization the structure-property-performance of N_2 fixation can be understood more clearly to guide further rational design of efficient catalysts.

Although solar-driven N_2 fixation activity has shown rapid development, from activities less than 100 to several thousand μmol/gh, it is believed that the gap between photo(electro)catalysis and Haber-Bosch thermal catalysis (several hundred mmol/gh)[71] is still huge, and the latter has been well known to produce huge amounts of NH_3 globally, which sustains the global food supply chain. We believe that the solar-driven N_2 fixation route might provide a new vista to fix N_2 and H_2O to NH_3 through less energy demanding and more green processes and also allow scientists to mimic and understand the nitrogenase enzyme structure.

C-C and S-S Coupling

Coupling reactions (such as C-C coupling and S-S coupling) are highly useful in the synthesis of new molecules, as well as for various medical, biological, materials, and nanotechnological applications. For instance, ethylene glycol derived from C-C coupling reactions is an important chemical with a production yield of over 25 million metric tons per year. It is produced from either the oil (oxidation of ethylene) or coal (hydrogenation of dimethyl oxalate) route. Traditionally, conversions of methanol involving C-C bond formation are restricted to dehydrative oligomerizations such as methanol-to-olefin and methanol-to-gasoline processes.[72,73] The preferential activation of inert sp3 α-C-H bonds in alcohol without affecting the hydroxyl group is highly challenging. Wang and Deng's team presented the first visible-light-driven dehydrogenative coupling of methanol to ethylene glycol using MoS_2 foam-CdS photocatalysts (Figures 5A and 5B).[74] An ethylene-glycol selectivity of 90% was obtained, with a yield of 16% and a quantum yield of above 5.0%. Mechanistic studies reveal that the preferential activation of the C-H bond in methanol is driven by photoexcited holes via a concerted proton-electron transfer mechanism on the CdS surfaces, forming a CH_2OH radical as an intermediate for C-C coupling and ethylene-glycol formation. The DFT calculations for methanol transformations on CdS indicate the weak adsorption of CH_3OH and CH_2OH intermediates on CdS, which decreases the possibility of O-H bond activation and enables the facile desorption of CH_2OH from catalyst surfaces for subsequent C-C coupling. However, in traditional thermal catalysis, a system that preferentially activates the C-H instead of O-H bond in methanol is very difficult to achieve. This exciting work reports a unique visible-light-driven catalytic C-H activation process, with the hydroxyl group in the molecule remaining intact.

Disulfides are also of interest as protecting groups in the synthesis of pharmaceuticals, bioactive compounds, or vulcanizing agents for rubbers.[75,76] Most of the methods to form S-S bonds involve metal-catalyzed or metal-free oxidative coupling of thiols. In addition to conventional oxidants such as manganese dioxide, dichromates, and chlorochromates, a number of new thermal methods employing cobalt-, manganese-, copper-, vanadium-, cerium-, and nickel-based catalysts have been reported for the aerobic oxidation of thiols into disulfides.[75,76] However, these methods are sub-optimal because of the toxicity and high cost of some of the metals. Thiols can also be easily over-oxidized to give undesired products such as sulfoxides and sulfones (Figure 5C path I). Thus, there is still great interest in developing clean, rapid, inexpensive, environmentally benign oxidative methods that can produce disulfides in high yields.

Wu and co-workers reported a simple, clean, and efficient photocatalytic (>400 nm) method for virtually quantitative and selective conversion of a variety of thiols into disulfides and molecular hydrogen.[77] This can be undertaken at room temperature using visible-light irradiation of CdSe-quantum dot (QD)-thiolate conjugates (path II in Figure 5C). When the water-soluble CdSe QDs are treated with acid, "vacant sites"

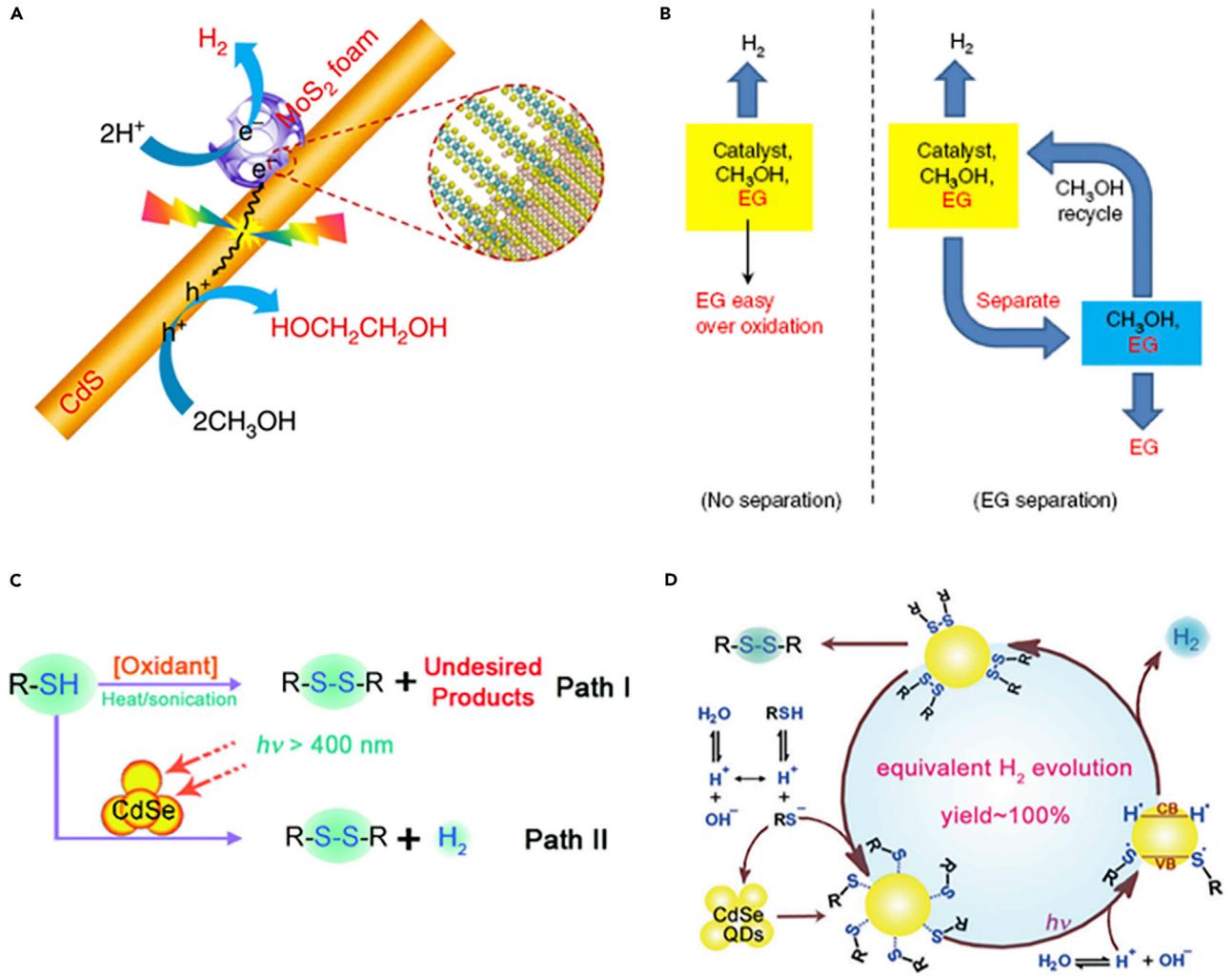

Figure 5. Photocatalytic C-C and S-S Coupling

(A) Schematic illustration of MoS_2 foam/CdS for photocatalytic synthesis of EG and H2 from CH_3OH.

(B) Conventional reaction mode and process-intensified mode with EG separation. Reproduced from Xie et al.,[74] with permission from Nature.

(C) Two general approaches for the conversion of thiols into disulfides.

(D) Proposed mechanism for the photocatalytic conversion of thiols into disulfides and molecular hydrogen. Reproduced from Li et al.,[77] with permission from Wiley-VCH.

are created on the surface of the QDs. The CdSe QDs bind the deprotonated thiols through cadmium-sulfur bonds to form QD-thiolate conjugates, and visible-light-induced electrons reduce the bound thiolates. This generates sulfur-centered radicals or radical-like species, which couple to form disulfides on the surface of the QDs (Figure 5D). Given that no sacrificial agent or oxidant is necessary and that the catalyst is reusable, this method may be attractive for the formation of disulfide bonds in other systems sensitive to the presence of oxidants. This is a rapidly developing field, and more visible-light-driven coupling processes are expected to emerge in the coming years.

Exploiting Natural Photosystems

Despite the many exciting developments in photocatalysis that have been achieved in the past 40 years, much can still be learned from naturally occurring catalytic processes, for instance, the photosynthetic splitting of water into oxygen and hydrogen.

Plants capture energy from the sun and store it in stable chemical bonds of organic molecules such as sugars and starch. Water oxidation is required for dioxygen evolution in both natural and artificial photosynthesis, and this process is catalyzed by the oxygen-evolving center (OEC). The core of the OEC in the natural photo-system II (PSII) consists of an asymmetric MnCa-O cluster bound to protein groups.[78,79] The natural photo-system may promote an insight into the structural and chemical determinants of biological water oxidation, which can lead to the development of superior catalysts for artificial photosynthesis (MnCaO-sites). Whether mononuclear Mn can also efficiently catalyze water oxidation has been a long-standing question.

Zhang and co-workers synthesized a Mn_4Ca-cluster similar to the native OEC, in terms of both the metal-oxygen core and the binding protein groups. Similar to the native OEC, the synthetic cluster can undergo four redox transitions and shows two magnetic resonance signals assignable to redox and structural isomerism (Figures 6A–6D).[80] Comparison with previously synthesized Mn_3CaO_4-cubane clusters suggests that the fourth Mn ion determines the redox potential and magnetic properties of the native OEC. Recently, Li et al. found that a heterogeneous catalyst with mononuclear manganese embedded in nitrogen-doped graphene (MnN-G) shows a turnover frequency as high as 214 s^{-1} for chemical water oxidation and had an electrochemical over-potential as low as 337 mV at a current density of 10 mA cm^{-2} (Figure 6E).[81] These values are close to the $CaMn_4O_5$ catalyst in photosystem II and two orders of magnitude higher than those of other Mn-based water oxidation catalysts.[81] Structural characterization and density functional theory calculations reveal that the high activity of Mn-NG can be attributed to the mononuclear manganese ion coordinated with four nitrogen atoms embedded in the graphene matrix.

Perspective and Challenge

The above sections show that energy from the sun is the most viable and economical solution to replace fossil fuels. Today's chemical industry is heavily reliant on fossil fuels and thus leads to abundant greenhouse gas (CO_2) emissions, as well as the production of contaminants such as NO_x, SO_x, VOC, and PM. Harnessing solar energy could potentially reduce the production of such pollutants. There have been major developments in solar-driven catalysis in the past few years, especially in C/N cycles for the synthesis of fuels and chemical feedstocks, and these hold the promise of producing such materials sustainably. However, such solar-driven technologies mainly hinge on the exploration of new photo(electro)/PV/photothermal catalysts. Compared with traditional thermal catalysis with a history of more than one century, there are still many issues to address before solar-driven catalysts can be widely adopted.

(1) The catalytic mechanism must be understood to allow the reactions to be controlled and produce desired products. The transient species involved are hard to detect, and there is a significant lack of understanding of the nature of the reaction intermediates. The exploration of the related transient absorption spectroscopy and excited-state DFT calculations may shed some light on the mechanisms by which solar-driven systems function.

(2) While recent reports of solar-driven CO or N_2 hydrogenation to olefins or ammonia in flow systems can give similar activity/selectivity to traditional thermal catalysis,[5,21] reactor design is still a major challenge. The lab irradiation sources used are usually Xe light with intensity 20–50 times greater than solar energy; thus, direct use of solar energy is still not possible. The use of a convex lens to focus solar energy restricts the size of the reactor, and natural day/night cycles and temperature variation pose challenges for industrial application. That

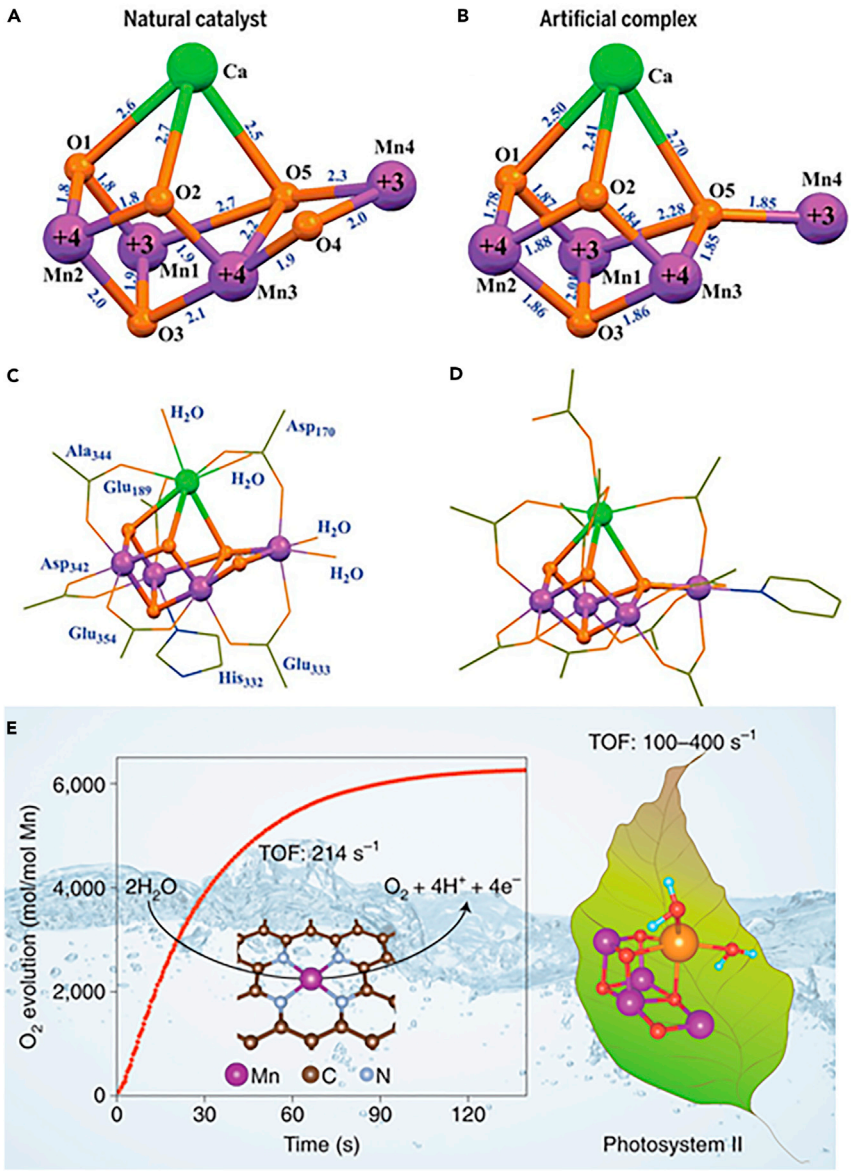

Figure 6. Natural Photosystems

Crystal structures of the native OEC and the synthetic Mn_4Ca complex (I) prepared by Zhang et al.[80]

(A) The Mn_4CaO_5 core of the native OEC.

(B) The Mn_4CaO_4 core of I.

(C) Structure of the native OEC, including ligating protein side chains and water molecules.

(D) Structure of I, including all ligand groups. Reproduced from Zhang et al.,[80] with permission from Nature.

(E) Time profile of O_2 evolution by a MnN-G-containing cluster in $Ce(NH_4)_2(NO_3)_6$ solution and the atomic model of the MnN_4-G cluster. Reproduced from Guan et al.,[81] with permission from Nature.

said, the idea of using this approach in the synthesis of higher-value fine chemicals (such as ethylene glycol[74] or asymmetric molecules[10]) in one-step vis photocatalysis warrants further investigation.

(3) Most photo(electro)catalyst materials show light absorption around 300–500 nm, with weak visible light absorption above 600 nm. Unfortunately, the latter makes up most of the energy of solar light; thus, catalysts that have the

ability to absorb the lower-energy region of the electromagnetic spectrum need to be developed. To this end, photothermal catalysts with a black color have been found to provide a potential pathway for the direct conversion of UV-VIS-IR light to heat for application in hydrogenation.

(4) The scale up and the cost of photo(electro/thermal) catalysts are critical for translation to pilot plants and use on the industrial scale since the solar source is restricted by the irradiation area and day/night cycle, etc. Loading a high amount of noble metals on a semiconductor is far from ideal, and the mild synthesis condition is advantageous from the industrial and economical point of view. Among the nanomaterials, LDHs represent one of the most promising materials for the further photo(electro/thermal) catalysis due to the ease of scale up and the tunable band structure.

In summary, the use of solar-energy-powered catalysis to facilitate bond breaking and formation on the surface of catalysts provides an exciting and sustainable pathway for future chemical synthesis. Ultimately, this may allow us to replace the standard thermal catalytic pathway in the selective activation of a range of species, ideally providing high catalytic efficacy and selectivity under mild conditions. The combination of photo, photoelectron, and/or photothermal catalysts with thermal catalysis is expected to contribute to a sustainable system for solar-driven catalysis and will make major contributions to global energy and environmental needs in the future.

ACKNOWLEDGMENTS

This work was financially supported by the National Key R&D Program of China (2017YFB0602200 and 2017YFB0307303), Natural Science Foundation of China (21725301, 21821004, 91645115, 21473003, 21878008, U1707603, 21625101, 21521005, and U1507102), Beijing Natural Science Foundation (2182047), and the Fundamental Research Funds for the Central Universities (XK1802-6, XK1902, and BUCTRC201807). We thank Zhifeng Hu (BUCT), Xingyi Qi (BUCT), and Xinglong Hu for their assistance in hand-drawing and designing some figures.

AUTHOR CONTRIBUTIONS

D.M. conceived this Perspective. Y.Z. and W.G. investigated the literature. Y.Z., W.G., and G.R.W. wrote the manuscript. Y.Z., W.G., G.R.W., A.H.M., S.L., and D.M. discussed and revised the manuscript.

REFERENCES

1. Shih, C.F., Zhang, T., Li, J., and Bai, C. (2018). Powering the future with liquid sunshine. Joule *2*, 1925.

2. Li, Z., Liu, J., Zhao, Y., Waterhouse, G.I.N., Chen, G., Shi, R., Zhang, X., Liu, X., Wei, Y., Wen, X.D., et al. (2018). Co-based catalysts derived from layered-double-hydroxide nanosheets for the photothermal production of light olefins. Adv. Mater. *30*, 1800527.

3. Schreier, M., Héroguel, F., Steier, L., Ahmad, S., Luterbacher, J.S., Mayer, M.T., Luo, J.S., and Grätzel, M. (2017). Solar conversion of CO_2 to CO using Earth-abundant electrocatalysts prepared by atomic layer modification of CuO. Nat. Energy *2*, 17087.

4. Zhao, Y., Li, B., Wang, Q., Gao, W., Wang, C.J., Wei, M., Evans, D.G., Duan, X., and O'Hare, D. (2014). NiTi-layered double hydroxides nanosheets as efficient photocatalysts for oxygen evolution from water using visible light. Chem. Sci. *5*, 951–958.

5. Zhao, Y., Li, Z., Li, M., Liu, J., Liu, X., Waterhouse, G.I.N., Wang, Y., Zhao, J., Gao, W., Zhang, Z., et al. (2018). Reductive transformation of layered-double-hydroxide nanosheets to Fe-based heterostructures for efficient visible-light photocatalytic hydrogenation of CO. Adv. Mater. *30*, 1803127.

6. Lei, F., Sun, Y., Liu, K., Gao, S., Liang, L., Pan, B., and Xie, Y. (2014). Oxygen vacancies confined in ultrathin indium oxide porous sheets for promoted visible-light water splitting. J. Am. Chem. Soc. *136*, 6826–6829.

7. Jiao, X., Chen, Z., Li, X., Sun, Y., Gao, S., Yan, W., Wang, C., Zhang, Q., Lin, Y., Luo, Y., et al. (2017). Defect-mediated electron-hole separation in one-unit-cell $ZnIn_2S_4$ layers for boosted solar-driven CO_2 reduction. J. Am. Chem. Soc. *139*, 7586–7594.

8. Li, H., Shang, J., Ai, Z.H., and Zhang, L.Z. (2015). Efficient visible light nitrogen fixation with BiOBr nanosheets of oxygen vacancies on the exposed {001} facets. J. Am. Chem. Soc. *137*, 6393–6399.

9. Li, J., Li, H., Zhan, G., and Zhang, L. (2017). Solar water splitting and nitrogen fixation with layered bismuth oxyhalides. Acc. Chem. Res. *50*, 112–121.

10. Liu, Q., and Wu, L.-Z. (2017). Recent advances in visible-light-driven organic reactions. Natl. Sci. Rev. *4*, 359–380.

11. Chen, C., Ma, W., and Zhao, J. (2010). Semiconductor-mediated photodegradation

of pollutants under visible-light irradiation. Chem. Soc. Rev. *39*, 4206–4219.

12. Boddy, P.J. (1968). Oxygen evolution on semiconding $TiO_{2[sub2]}$. J. Electrochem. Soc. *115*, 199.

13. Fujishima, A., and Honda, K. (1972). Electrochemical photolysis of water at a semiconductor electrode. Nature *238*, 37–38.

14. Grätzel, M. (2001). Photoelectrochemical cells. Nature *414*, 338–344.

15. Wu, X., Lu, G.Q., and Wang, L. (2011). Shell-in-shell TiO_2 hollow spheres synthesized by one-pot hydrothermal method for dye-sensitized solar cell application. Energy Environ. Sci. *4*, 3565.

16. Grätzel, M. (2014). The light and shade of perovskite solar cells. Nat. Mater. *13*, 838–842.

17. Luo, J., Im, J.H., Mayer, M.T., Schreier, M., Nazeeruddin, M.K., Park, N.G., Tilley, S.D., Fan, H.J., and Grätzel, M. (2014). Water photolysis at 12.3% efficiency *via* perovskite photovoltaics and earth-abundant catalysts. Science *345*, 1593–1596.

18. Meng, X., Liu, L., Ouyang, S., Xu, H., Wang, D., Zhao, N., and Ye, J. (2016). Nanometals for solar-to-chemical energy conversion: from semiconductor-based photocatalysis to plasmon-mediated photocatalysis and photo-thermocatalysis. Adv. Mater. Weinheim *28*, 6781–6803.

19. Liu, G., Meng, X., Zhang, H., Zhao, G., Pang, H., Wang, T., Li, P., Kako, T., and Ye, J. (2017). Elemental boron for efficient carbon dioxide reduction under light irradiation. Angew. Chem. Int. Ed. Engl. *56*, 5570–5574.

20. Ren, J., Ouyang, S., Xu, H., Meng, X., Wang, T., Wang, D., and Ye, J. (2017). Targeting activation of CO_2 and H_2 over Ru-loaded ultrathin layered double hydroxides to achieve efficient photothermal CO_2 methanation in flow-type system. Adv. Energy Mater. *7*, 1601657.

21. Mao, C.L., Yu, L.H., Li, J., Zhao, J.C., and Zhang, L.Z. (2018). Energy-confined solar thermal ammonia synthesis with $K/Ru/TiO_{2-x}H_x$. Appl. Catal. B Environ. *224*, 612–620.

22. Zeng, M., Li, Y., Mao, M., Bai, J., Ren, L., and Zhao, X. (2015). Synergetic effect between photocatalysis on TiO_2 and thermocatalysis on CeO_2 for gas-phase oxidation of benzene on TiO_2/CeO_2 nanocomposites. ACS Catal. *5*, 3278–3286.

23. Yin, Z., Wang, Y., Song, C., Zheng, L., Ma, N., Liu, X., Li, S., Lin, L., Li, M., Xu, Y., et al. (2018). Hybrid Au-Ag nanostructures for enhanced plasmon-driven catalytic selective hydrogenation through visible light irradiation and surface-enhanced Raman scattering. J. Am. Chem. Soc. *140*, 864–867.

24. Zhou, L.A., Swearer, D.F., Zhang, C., Robatjazi, H., Zhao, H.Q., Henderson, L., Dong, L.L., Christopher, P., Carter, E.A., Nordlander, P., et al. (2018). Quantifying hot carrier and thermal contributions in plasmonic photocatalysis. Science *362*, 69–72.

25. Tian, Y., and Tatsuma, T. (2005). Mechanisms and applications of plasmon-induced charge separation at TiO_2 films loaded with gold nanoparticles. J. Am. Chem. Soc. *127*, 7632–7637.

26. Liu, G.G., Li, P., Zhao, G.X., Wang, X., Kong, J.T., Liu, H.M., Zhang, H.B., Chang, K., Meng, X.G., Kako, T., et al. (2016). Promoting active species generation by plasmon-induced hot-electron excitation for efficient electrocatalytic oxygen evolution. J. Am. Chem. Soc. *138*, 9128–9136.

27. Huang, H., Zhang, L., Lv, Z.H., Long, R., Zhang, C., Lin, Y., Wei, K.C., Wang, C.M., Chen, L., Li, Z.Y., et al. (2016). Unraveling surface plasmon decay in core-shell nanostructures toward broadband light-driven catalytic organic synthesis. J. Am. Chem. Soc. *138*, 6822–6828.

28. Jiang, D., Wang, W., Sun, S., Zhang, L., and Zheng, Y. (2015). Equilibrating the plasmonic and catalytic roles of metallic nanostructures in photocatalytic oxidation over Au. modified CeO_2. ACS Catal. *5*, 613.

29. Schlögl, R. (2010). The role of chemistry in the energy challenge. ChemSusChem *3*, 209–222.

30. Chen, J.G., Crooks, R.M., Seefeldt, L.C., Bren, K.L., Bullock, R.M., Darensbourg, M.Y., Holland, P.L., Hoffman, B., Janik, M.J., Jones, A.K., et al. (2018). Beyond fossil fuel-driven nitrogen transformations. Science *360*, 873.

31. Yao, S., Zhang, X., Zhou, W., Gao, R., Xu, W., Ye, Y., Lin, L., Wen, X., Liu, P., Chen, B., et al. (2017). Atomic-layered Au clusters on alpha-MoC as catalysts for the low-temperature water-gas shift reaction. Science *357*, 389–393.

32. Tang, P., Zhu, Q.J., Wu, Z.X., and Ma, D. (2014). Methane activation: the past and future. Energy Environ. Sci. *7*, 2580–2591.

33. Yuliati, L., and Yoshida, H. (2008). Photocatalytic conversion of methane. Chem. Soc. Rev. *37*, 1592–1602.

34. Guo, X.G., Fang, G.Z., Li, G., Ma, H., Fan, H.J., Yu, L., Ma, C., Wu, X., Deng, D.H., Wei, M.M., et al. (2014). Direct, nonoxidative conversion of methane to ethylene, aromatics, and hydrogen. Science *344*, 616–619.

35. Kato, Y., Yoshida, H., and Hattori, T. (1998). Photoinduced non-oxidative coupling of methane over silica-alumina and alumina around room temperature. Chem. Commun. 2389.

36. Li, L., Li, G.D., Yan, C., Mu, X.Y., Pan, X.L., Zou, X.X., Wang, K.X., and Chen, J.S. (2011). Efficient sunlight-driven dehydrogenative coupling of methane to ethane over a Zn^+-modified zeolite. Angew. Chem. Int. Ed. *50*, 8299–8303.

37. Li, L., Cai, Y.Y., Li, G.D., Mu, X.Y., Wang, K.X., and Chen, J.S. (2012). Synergistic effect on the photoactivation of the methane C-H bond over Ga(3+)-modified ETS-10. Angew. Chem. Int. Ed. Engl. *51*, 4702–4706.

38. Li, L., Fan, S.Z., Mu, X.Y., Mi, Z.T., and Li, C.J. (2014). Photoinduced conversion of methane into benzene over GaN nanowires. J. Am. Chem. Soc. *136*, 7793–7796.

39. Li, W., He, D., Hu, G., Li, X., Banerjee, G., Li, J., Lee, S.H., Dong, Q., Gao, T., Brudvig, G.W., et al. (2018). Selective CO production by photoelectrochemical methane oxidation on TiO_2. ACS Cent. Sci. *4*, 631–637.

40. Huang, H., Mao, M.Y., Zhang, Q., Li, Y.Z., Bai, J.L., Yang, Y., Zeng, M., and Zhao, X.J. (2018). Solar-light-driven CO_2 reduction by CH_4 on silica-cluster-modified Ni nanocrystals with a high solar-to-fuel efficiency and excellent durability. Adv. Energy Mater *8*, 1702472.

41. Song, H., Meng, X., Wang, Z.-j., Wang, Z., Chen, H., Weng, Y., Ichihara, F., Oshikiri, M., Kako, T., and Ye, J. (2018). Visible-light-mediated methane activation for steam methane reforming under mild conditions: a case study of Rh/TiO_2 catalysts. ACS Catal. *8*, 7556–7565.

42. Cui, X.J., Li, H.B., Wang, Y., Hu, Y.L., Hua, L., Li, H.Y., Han, X.W., Liu, Q.F., Yang, F., He, L.M., et al. (2018). Room-temperature methane conversion by graphene-confined single iron atoms. Chem *4*, 1902.

43. Xie, J.J., Jin, R.X., Li, A., Bi, Y.P., Ruan, Q.S., Deng, Y.C., Zhang, Y.J., Yao, S.Y., Sankar, G., Ma, D., et al. (2018). Highly selective oxidation of methane to methanol at ambient conditions by titanium dioxide-supported iron species. Nat Catal. *1*, 889–896.

44. Schmidt, R.J. (2005). Industrial catalytic processes—phenol production. Appl. Catal. A Gen. *280*, 89–103.

45. Niwa Si, S., Eswaramoorthy, M., Nair, J., Raj, A., Itoh, N., Shoji, H., Namba, T., and Mizukami, F. (2002). A one-step conversion of benzene to phenol with a palladium membrane. Science *295*, 105–107.

46. Zhou, Y., Ma, Z., Tang, J., Yan, N., Du, Y., Xi, S., Wang, K., Zhang, W., Wen, H., and Wang, J. (2018). Immediate hydroxylation of arenes to phenols *via* V-containing all-silica ZSM-22 zeolite triggered non-radical mechanism. Nat. Commun. *9*, 2931.

47. Ide, Y., Torii, M., and Sano, T. (2013). Layered silicate as an excellent partner of a TiO_2 photocatalyst for efficient and selective green fine-chemical synthesis. J. Am. Chem. Soc. *135*, 11784–11786.

48. Zheng, Y.W., Chen, B., Ye, P., Feng, K., Wang, W., Meng, Q.Y., Wu, L.Z., and Tung, C.H. (2016). Photocatalytic hydrogen-evolution cross-couplings: benzene C–H amination and hydroxylation. J. Am. Chem. Soc. *138*, 10080–10083.

49. Sastre, F., Puga, A.V., Liu, L., Corma, A., and García, H. (2014). Complete photocatalytic reduction of CO_2 to methane by H_2 under solar light irradiation. J. Am. Chem. Soc. *136*, 6798–6801.

50. Sastre, F., Corma, A., and García, H. (2013). Visible-light photocatalytic conversion of carbon monoxide to methane by nickel(II) oxide. Angew. Chem. Int. Ed. Engl. *52*, 12983–12987.

51. Meng, X., Wang, T., Liu, L., Ouyang, S., Li, P., Hu, H., Kako, T., Iwai, H., Tanaka, A., and Ye, J. (2014). Photothermal conversion of CO_2 into CH_4 with H_2 over group VIII nanocatalysts: an alternative approach for solar fuel production. Angew. Chem. Int. Ed. *53*, 11478–11482.

52. Chen, G., Gao, R., Zhao, Y., Li, Z., Waterhouse, G.I.N., Shi, R., Zhao, J., Zhang, M., Shang, L., Sheng, G., et al. (2018). Alumina-supported CoFe alloy catalysts derived from layered-double-hydroxide nanosheets for efficient

photothermal CO_2 hydrogenation to hydrocarbons. Adv. Mater. *30*, 1704663.

53. Zhai, P., Xu, C., Gao, R., Liu, X., Li, M., Li, W., Fu, X., Jia, C., Xie, J., Zhao, M., et al. (2016). Highly tunable selectivity for syngas-derived alkenes over zinc and sodium-modulated Fe_5C_2 catalyst. Angew. Chem. Int. Ed. *55*, 9902–9907.

54. Zhao, B., Zhai, P., Wang, P., Li, J., Li, T., Peng, M., Zhao, M., Hu, G., Yang, Y., Li, Y.-W., et al. (2017). Direct transformation of syngas to aromatics over Na-Zn-Fe_5C_2 and hierarchical HZSM-5 tandem catalysts. Chem *3*, 323–333.

55. Zhao, Y., Zhao, B., Liu, J., Chen, G., Gao, R., Yao, S., Li, M., Zhang, Q., Gu, L., Xie, J., et al. (2016). Oxide-modified nickel photocatalysts for the production of hydrocarbons in visible light. Angew. Chem. Int. Ed. Engl. *55*, 4215–4219.

56. Gao, W., Gao, R., Zhao, Y., Peng, M., Song, C., Li, M., Li, S., Liu, J., Li, W., Deng, Y., et al. (2018). Photo-driven syngas conversion to lower olefins over oxygen-decorated Fe_5C_2 catalyst. Chem *4*, 2917–2928.

57. Wang, L., Xia, M.K., Wang, H., Huang, K.F., Qian, C.X., Maravelias, C.T., and Ozin, G.A. (2018). Greening ammonia toward the solar ammonia refinery. Joule *2*, 1055–1074.

58. Kitano, M., Inoue, Y., Yamazaki, Y., Hayashi, F., Kanbara, S., Matsuishi, S., Yokoyama, T., Kim, S.W., Hara, M., and Hosono, H. (2012). Ammonia synthesis using a stable electride as an electron donor and reversible hydrogen store. Nat. Chem. *4*, 934–940.

59. Gong, Y., Wu, J., Kitano, M., Wang, J., Ye, T.-N., Li, J., Kobayashi, Y., Kishida, K., Abe, H., Niwa, Y., et al. (2018). Ternary intermetallic LaCoSi as a catalyst for N_2 activation. Nat Catal. *1*, 178–185.

60. Wang, P.K., Chang, F., Gao, W.B., Guo, J.P., Wu, G.T., He, T., and Chen, P. (2017). Breaking Scaling relations to achieve low-temperature ammonia synthesis through LiH-mediated nitrogen transfer and hydrogenation. Nat. Chem. *9*, 64–70.

61. Gao, W.B., Guo, J.P., Wang, P.K., Wang, Q.R., Chang, F., Pei, Q.J., Zhang, W.J., Liu, L., and Chen, P. (2018). Production of ammonia *via* a chemical looping process based on metal imides as nitrogen carriers. Nat. Energy *3*, 1067–1075.

62. Wang, S., Hai, X., Ding, X., Chang, K., Xiang, Y., Meng, X., Yang, Z., Chen, H., and Ye, J. (2017). Light-switchable oxygen vacancies in ultrafine Bi_5O_7Br nanotubes for boosting solar-driven nitrogen fixation in pure water. Adv. Mater. *29*, 1701774.

63. Zhang, N., Jalil, A., Wu, D.X., Chen, S.M., Liu, Y.F., Gao, C., Ye, W., Qi, Z.M., Ju, H.X., Wang, C.M., et al. (2018). Refining defect states in $W_{18}O_{49}$ by Mo doping: a strategy for tuning N_2 activation towards solar-driven nitrogen fixation. J. Am. Chem. Soc. *140*, 9434–9443.

64. Hirakawa, H., Hashimoto, M., Shiraishi, Y., and Hirai, T. (2017). Photocatalytic conversion of nitrogen to ammonia with water on surface oxygen vacancies of titanium dioxide. J. Am. Chem. Soc. *139*, 10929–10936.

65. Zhao, Y., Zhao, Y., Waterhouse, G.I.N., Zheng, L., Cao, X., Teng, F., Wu, L.Z., Tung, C.H., O'Hare, D., and Zhang, T. (2017). Layered-double-hydroxide nanosheets as efficient visible-light-driven photocatalysts for dinitrogen fixation. Adv. Mater. *29*, 1703828.

66. Yang, J.H., Guo, Y.Z., Jiang, R.B., Qin, F., Zhang, H., Lu, W.Z., Wang, J.F., and Yu, J.C. (2018). High-efficiency "working-in-tandem" nitrogen photofixation achieved by assembling plasmonic gold nanocrystals on ultrathin Titania nanosheets. J. Am. Chem. Soc. *140*, 8497–8508.

67. Li, C.C., Wang, T., Zhao, Z.J., Yang, W.M., Li, J.F., Li, A., Yang, Z.L., Ozin, G.A., and Gong, J.L. (2018). Promoted fixation of molecular nitrogen with surface oxygen vacancies on plasmon-enhanced TiO_2 photoelectrodes. Angew. Chem. Int. Ed. Engl. *57*, 5278–5282.

68. Meng, L.S., Chen, Z.Y., Ma, Z.Y., He, S., Hou, Y.D., Li, H.H., Yuan, R.S., Huang, X.H., Wang, X.X., Wang, X.C., et al. (2018). Gold plasmon-induced photocatalytic dehydrogenative coupling of methane to ethane on polar oxide surfaces. Energy Environ. Sci. *11*, 294–298.

69. Zhang, X., Li, X., Zhang, D., Su, N.Q., Yang, W., Everitt, H.O., and Liu, J. (2017). Product selectivity in plasmonic photocatalysis for carbon dioxide hydrogenation. Nat. Commun. *8*, 14542.

70. Yang, X., Nash, J., Anibal, J., Dunwell, M., Kattel, S., Stavitski, E., Attenkofer, K., Chen, J.G., Yan, Y., and Xu, B. (2018). Mechanistic insights into electrochemical nitrogen reduction reaction on vanadium nitride nanoparticles. J. Am. Chem. Soc. *140*, 13387–13391.

71. Kitano, M., Inoue, Y., Ishikawa, H., Yamagata, K., Nakao, T., Tada, T., Matsuishi, S., Yokoyama, T., Hara, M., and Hosono, H. (2016). Essential role of hydride ion in ruthenium-based ammonia synthesis catalysts. Chem. Sci. *7*, 4036–4043.

72. Maitlis, P.M., Haynes, A., Sunley, G.J., and Howard, M.J. (1996). Methanol carbonylation revisited: thirty years on. J. Chem. Soc., Dalton Trans. *11*, 2187.

73. Olsbye, U., Svelle, S., Bjørgen, M., Beato, P., Janssens, T.V.W., Joensen, F., Bordiga, S., and Lillerud, K.P. (2012). Conversion of methanol to hydrocarbons: how zeolite cavity and pore size controls product selectivity. Angew. Chem. Int. Ed. Engl. *51*, 5810–5831.

74. Xie, S., Shen, Z., Deng, J., Guo, P., Zhang, Q., Zhang, H., Ma, C., Jiang, Z., Cheng, J., Deng, D., et al. (2018). Visible light-driven C-H activation and C-C coupling of methanol into ethylene glycol. Nat. Commun. *9*, 1181.

75. García Ruano, J.L., Parra, A., and Alemán, J. (2008). Efficient synthesis of disulfides by air oxidation of thiols under sonication. Green Chem. *10*, 706.

76. Dou, Y., Huang, X., Wang, H., Yang, L., Li, H., Yuan, B., and Yang, G. (2017). Reusable cobalt-phthalocyanine in water: efficient catalytic aerobic oxidative coupling of thiols to construct S–N/S–S bonds. Green Chem. *19*, 2491–2495.

77. Li, X.B., Li, Z.J., Gao, Y.J., Meng, Q.Y., Yu, S., Weiss, R.G., Tung, C.H., and Wu, L.Z. (2014). Mechanistic insights into the interface-directed transformation of thiols into disulfides and molecular hydrogen by visible-light irradiation of quantum dots. Angew. Chem. Int. Ed. Engl. *53*, 2085–2089.

78. Yano, J., and Yachandra, V. (2014). Mn_4Ca cluster in photosynthesis: where and how water is oxidized to dioxygen. Chem. Rev. *114*, 4175–4205.

79. Ogata, K., Yuki, T., Hatakeyama, M., Uchida, W., and Nakamura, S. (2013). All-atom molecular dynamics simulation of photosystem II embedded in thylakoid membrane. J. Am. Chem. Soc. *135*, 15670–15673.

80. Zhang, C.X., Chen, C.H., Dong, H.X., Shen, J.R., Dau, H., and Zhao, J.Q. (2015). Inorganic chemistry. A synthetic Mn_4Ca-cluster mimicking the oxygen-evolving center of photosynthesis. Science *348*, 690–693.

81. Guan, J.Q., Duan, Z.Y., Zhang, F.X., Kelly, S.D., Si, R., Dupuis, M., Huang, Q.G., Chen, J.Q., Tang, C.H., and Li, C. (2018). Water oxidation on a mononuclear manganese heterogeneous catalyst. Nat Catal. *1*, 870–877.